# Distribution functions of coexisting phases in a complete solid solution system

Wenwu Cao and L. Eric Cross
*Materials Research Laboratory, The Pennsylvania State University, University Park, Pennsylvania 16802*

(Received 18 June 1992; accepted for publication 8 December 1992)

In the phase diagram of a binary system one often encounters a compositional region in which two phases coexist. A common practice is to use the Lever Rule to describe the distributions of the two coexisting phases. However, if the binary system is a complete solid solution system, the Lever Rule cannot be used. A new type of distribution has been derived for a solid solution system without solubility gap. Application of the theory to pure and modified lead-zirconate–lead-titanate (PZT) systems shows excellent agreement with the experimental data. Several disputed facts about PZT are also explained satisfactorily.

## I. INTRODUCTION

A general phase diagram of a binary system A-B is given in Fig. 1(a). There is one liquid phase $L$ and two solid solutions $\alpha$ and $\gamma$. A and B are completely miscible in the liquid phase, but in the solid phase there is a solubility gap in which the two solid solutions $\alpha$ and $\gamma$ coexist. At temperature $T_1$, for any composition $x$ inside the solubility gap, $g<x<h$, the molar percentages $f_\alpha$ and $f_\gamma$ of the two coexisting phases are governed by the Lever Rule,

$$f_\alpha : f_\gamma = \overline{xh} : \overline{gx}, \qquad f_\alpha + f_\gamma = 1. \tag{1}$$

The two special points $g$ and $h$ on the isothermal tieline at $T=T_1$ represent the boundaries of the solubility gap. The corresponding free-energy versus composition plot is shown in Fig. 1(b). One can see that the two boundary compositions $g$ and $h$ are located at the common tangent points of the two free energies for the $\alpha$ and $\gamma$ phases. For compositions falling inside this solubility gap, two-phase mixtures will be formed consisting of $g$ and $h$ compositions, with the ratio of the two phases obeying the Lever Rule [Eq. (1)].

Figure 1(c) is another type of phase diagram for an A-B binary compound. Looking at the subsolidus region we have three solid solutions, $\beta$, $\alpha$, and $\gamma$. This is a complete solid solution system, viz., no miscibility gaps and no solubility gaps; however, there is a structural phase transition from $\beta$ to either $\alpha$ or $\gamma$ phase depending on the composition of the solid solution. The well-known lead zirconate titanate (PZT) and its derivatives are examples of this situation. For this system, the free energies of $\alpha$ and $\beta$ phases are monotonic functions of composition. Because there are no chemical decompositions in the complete solid solution system, for simplicity we only consider the relative stability of the $\alpha$ and $\beta$ phases. We know that in this system, the difference of the two low-temperature phases is characterized by the polarization which is the primary order parameter in the paraelectric-ferroelectric phase transition; hence, to analyze the relative stability we only need to know the free energy associated with the polarization. Using Landau–Devonshire type phenomenological theory, the compositional dependence of the free energies associated with the polarization for the $\alpha$ and $\beta$ phases may be drawn as in Fig. 1(d) at $T_1$.[1] One can see from Fig. 1(d) that the coexistence of the $\alpha$ and $\gamma$ phases should be allowed only for one composition $k$, but not for a finite compositional region according to thermodynamics.

To some extent, Fig. 1(d) may be deceiving at first glance, because if the composition is taken as an independent variable, the transition from $\alpha$ to $\gamma$ is obviously first order and the transition hysteresis with respect to the change of composition will result in a coexistence region. In fact, this is one of the explanations given for the coexistence region found in the PZT system.[2] Unfortunately, the composition cannot be changed in the subsolidus temperature region. Once a compound is formed at much higher temperature ($>800$ °C), the composition variable is frozen in the subsolidus region. The polarization related free energy for each phase at $T_1$ [Fig. 1(d)] is obtained independently for each composition from the corresponding prototype phase following the change of temperature. Therefore, in order to study this problem we must look at the temperature-induced phase transition from $\beta$ to $\alpha$ and $\beta$ to $\gamma$.

From Fig. 1(d) we can see that both free energies for the $\alpha$ and $\gamma$ phases are monotonic functions of composition, and there is one crossover point $k$ which is termed the morphotropic phase boundary (MPB). From energy minimization principles only one phase is stable in the low-temperature region for any given composition, which is to say that at $T_c$ the $\beta$ phase will be transformed into either the $\alpha$ or $\gamma$ phase depending on the composition of the solid solution. However, when the transition temperature is reasonably high and the phase transition from $\beta$ to $\alpha$ or $\gamma$ is of second order, thermal energy could induce some amount of the second metastable phase at the transition, especially when the difference of the free energies of the two low-temperature phases is small, such as for those compositions near the MPB [see Fig. 1(d)]. It is our opinion that the phase coexistence observed in the PZT system near the MPB is the result of a frozen-in second metastable phase as elaborated below.

One must note that the phase mixing is completely different in the cases of Figs. 1(a) and 1(c). In the former

 0021-8979/93/073250-06$06.00  

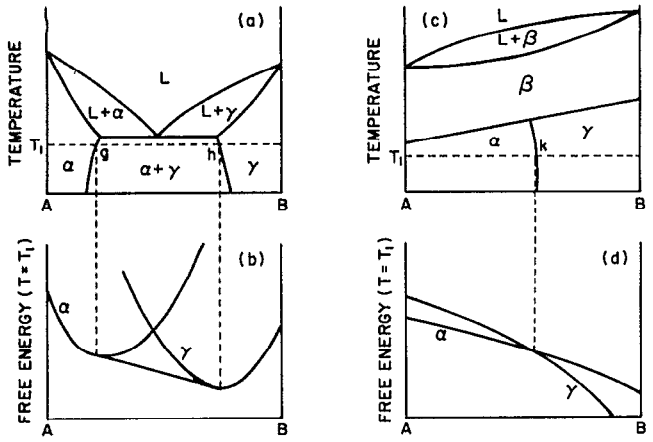


FIG. 1. Phase diagram for a binary A-B system. (a) Solid solutions $\alpha$ and $\gamma$ coexist inside the solubility gap in the subsolidus region. (b) The free energies of $\alpha$ and $\gamma$ phases vs composition at temperature $T_1$. The two tangent points correspond to the edge compositions of the solubility gap. (c) Phase diagram for a complete solid solution system. The nearly vertical line that divides the $\alpha$ and $\gamma$ phase is the morphotropic phase boundary. (d) The change of the free energy related to the polarization with respect to composition at temperature $T_1$ for both the $\alpha$ and $\gamma$ phases in the complete solid solution system described in (c).

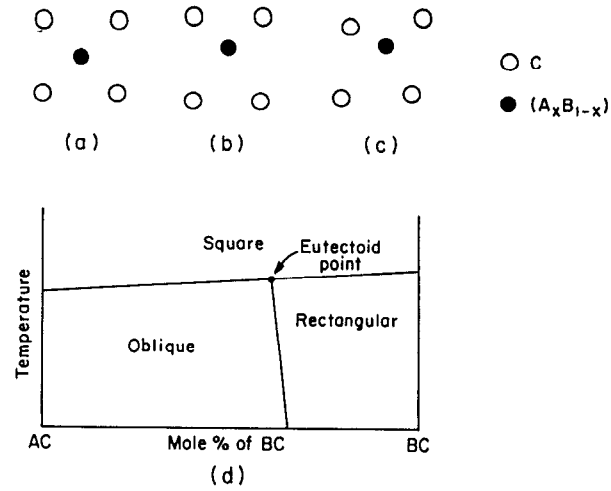


FIG. 2. Illustration of two-dimensional square-rectangular and square-oblique structural phase transitions in a complete solid solution AC-BC. (a), (b), and (c) are the lattice structures for the paraelectric square, ferroelectric rectangular, and ferroelectric oblique phases, respectively; (d) is the corresponding phase diagram.

we mix two phases of different structures and of different chemical compositions but in the latter we mix two different structures of the same chemical composition. Because of the different chemical compositions in the former case, the conservation of matter leads to the Lever Rule. But for the case in Fig. 1(c), the distribution functions cannot be obtained straightforwardly because the condition of identical chemical composition invalidates the arguments used to derive the Lever Rule.

A new approach has been proposed to calculate the partitioning of the rhombohedral and tetragonal phases at the MPB when the structural phase transition from $\beta$ to $\alpha$ or $\gamma$ is of second order.[3] Here we will try to extend that model to address the phase coexistence near the MPB in a complete solid solution system by incorporating classical statistics. This proposed theory is applicable to the PZT system because the paraelectric-ferroelectric phase transitions for PZT solid solutions of composition near the MPB are indeed second order.[4]

## II. THEORY

For simplicity, we will study a statistical ensemble of independent particles, for example, a ceramic powder system or even (to first-order approximation) a ceramic system (an ensemble of grains) may be considered to be such ensembles. For each particle, we assume it is a single-phase system both before and after the phase transition. In what follows we will calculate the probabilities of one of the particles transforming from the high-temperature phase $\beta$ into one of the low-temperature phases $\alpha$ or $\gamma$, and use these probability functions as the new distribution functions for the statistical ensemble with compositions near the MPB.

In order to visualize the concept let us look at a hypothesized 2D problem of a complete solid solution system AC-BC. The high-temperature phase is a nonferroelectric square phase as shown in Fig. 2(a) and the two low-temperature phases are rectangular and oblique ferroelectric phases as shown in Figs. 2(b) and 2(c), respectively. The phase diagram in the subsolidus region is given in Fig. 2(d). For convenience we call the starting point of the morphotropic phase boundary the "eutectoid point."

Assuming that the phase transition from the square phase to either the oblique or rectangular phase is second order near the eutectoid point, strong thermal fluctuations will occur near the transition temperature $T_c$. Sufficiently below $T_c$ the system will be frozen into one of the low-temperature phases. In a way we are dealing with a "quenching" problem from the fluctuating state to a ferroelectric state. Hence, the probabilities of transforming from the square to the rectangular or oblique phases are predetermined in the fluctuating state. This situation is depicted in Fig. 3. The profile of the fluctuating state near $T_c$ and the final low-temperature states are shown in Figs. 3(a) and 3(b), respectively, in the order parameter space. The

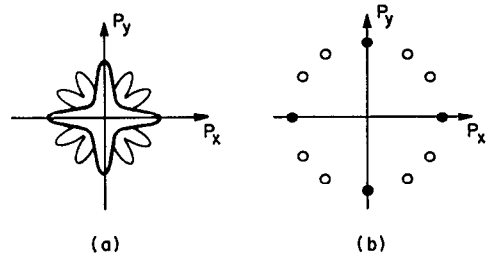


FIG. 3. (a) Thermal fluctuation profile at the eutectoid point in the order parameter space for the two-dimensional problem described in Fig. 2. (b) Degenerate low-temperature states for the morphotropic phase boundary composition: (●) rectangular phase; (○) oblique phase.

thicker line in Fig. 3(a) illustrates the profile for the case of square-rectangular transition [near the BC end of the composition region in Fig. 2(d)] and the thinner line is for the case of square-oblique transition [near the AC end of the composition region in Fig. 2(d)]. In the compositional region near the eutectoid point, the profile of the fluctuation will look like the outer rim of the pattern in Fig. 3(a).

There is a link between the situations described in Figs. 3(a) and 3(b), which becomes apparent if we assume that the thermal fluctuations have no orientational preference. In other words, although the magnitude of the fluctuation is regulated by the potential well, the orientation probability of thermally induced instant polarization $\mathbf{P}_{ist}$ should have no directional preference. Thus the probability of attaining a particular low-temperature state in Fig. 3(b) on cooling from the fluctuating state [Fig. 3(a)] is proportional to the effective angle that state corresponds to in the fluctuating state. A polygon may be constructed to calculate the effective angle of each low-temperature state in the 2D problem where each edge of the polygon subtends an effective angle for each of the low temperature states. An important task is to define the boundaries between these effective angles. A method for defining the boundary has been given when the low-temperature states are degenerate.[3] Considering the picture in Fig. 3(a), if $\mathbf{P}_{ist}$ is oriented inside a particular angular region while being frozen into the low-temperature phase, the final state should be one of the states in Fig. 3(b) whose polarization has the smallest angle with $\mathbf{P}_{ist}$. Therefore, the probability of becoming one of the states in Fig. 3(b) on cooling from the fluctuating state is equal to a corresponding effective angle in Fig. 3(a) divided by $2\pi$—the normalization constant.

This concept can be easily generalized to a three-dimensional case, for which the probability of attaining a low-temperature state when frozen from the fluctuating state is proportional to a corresponding effective solid angle divided by $4\pi$. For the three-dimensional case, a polyhedron may be constructed in the order parameter space to calculate these effective solid angles; it has been named the "probability polyhedron."[3]

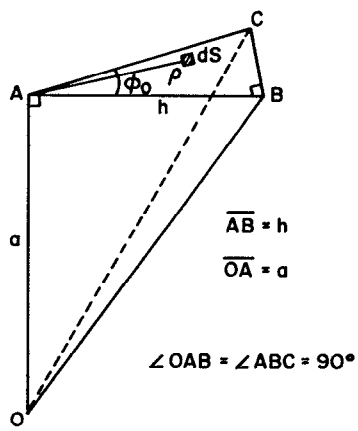


FIG. 4. Solid angle subtended by a right-angle surface ◁ABC with respect to the point O.

The solid angle calculations may be carried out on the surface of the polyhedron. Utilizing the relatively high symmetry of the problem, we only need to derive a general formula for the solid angle subtended by a right triangle surface as shown in Fig. 4; the solid angle is given by

$$\Omega_{OABC}=\iint_{\triangleleft ABC}\frac{a\,ds}{(\rho^2+a^2)^{3/2}}, \tag{2}$$

where $ds$ is the area element on the surface of ◁ABC and $\rho$ is the distance of this area element from point A. The integration may be conveniently carried out using cylindrical coordinates

$$\begin{aligned}\Omega_{OABC}&=a\phi_0\int_0^h\frac{\rho\,d\rho}{(\rho^2+a^2)^{3/2}}\\&\quad+a\int_h^{h/\cos\phi_0}\frac{\phi_0-\arccos(h/\rho)\,\rho\,d\rho}{(a^2+\rho^2)^{3/2}}\\&=\phi_0-\frac{\pi}{4}-\frac{1}{2}\arcsin\left(\frac{1-2\cos^2\phi_0-(h/a)^2}{1+(h/a)^2}\right).\end{aligned} \tag{3}$$

For the study of the coexistence of nondegenerate

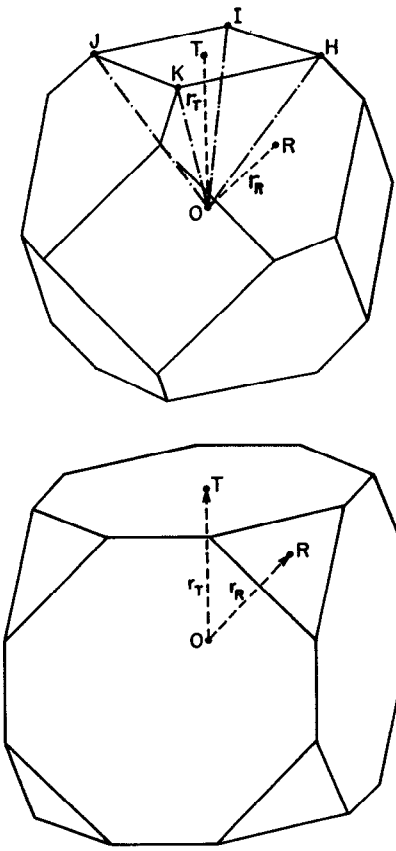


FIG. 5. Probability polyhedron for complete solid solution systems with coexisting rhombohedral and tetragonal phases, such as PZT, with the parameter $\delta$ in the ranges (a) $1-\sqrt{3}<\delta<1-(2/\sqrt{3})$ and (b) $1-(2/\sqrt{3})<\delta<1-(1/\sqrt{3})$.

states, we use the following arguments to define the boundaries between different effective solid angles in the fluctuating states.

(i) At $T_c$ the thermal energy is of the order of $kT_c$, so that there are probabilities for the non-lowest-energy states to be occupied; this probability is proportional to $\exp[-(G_i-G_L)/kT_c]$, where $G_i$ and $G_L$ are the free energies of the $i$th low-temperature state and the ground (lowest free energy) state, respectively. Here we have assumed that configurational tunneling near $T_c$ is allowed to achieve global equilibrium, because the system is very "soft" near $T_c$.

(ii) The solid angle $\Omega_i$ subtended by a given surface area with respect to a fixed point in space is inversely proportional to the square of the distance $r_i$ between this surface and that point.

Since the solid angle $\Omega_i$ is equivalent to the probability of attaining the $i$th low-temperature state, using the arguments (i) and (ii) above we may assume the following relationship between the distance variable $r_i$ and the free energies:

$$r_i \propto \frac{1}{\sqrt{\Omega_i}} \propto \exp\left(\frac{G_i-G_L}{2kT_c}\right). \tag{4}$$

It can be proved that only one parameter $\delta$ is needed to calculate a binary system, such as the PZT system, where $\delta$ is the relative distance,

$$\delta=\frac{r_T-r_R}{r_T}=1-\exp\left(\frac{G_R-G_T}{2kT_c}\right). \tag{5}$$

$G_R$ and $G_T$ are the free energies of the rhombohedral and tetragonal phases, respectively.

The probability polyhedron for the PZT system is given in Figs. 5(a) and 5(b). One must note that the representative surfaces for the rhombohedral and tetragonal phases change their shape for $\delta>1-(2/\sqrt{3})$ and $\delta<1-(2/\sqrt{3})$. When $r_R>\sqrt{3}r_T$, the six representative surfaces for the tetragonal phase will meet each other to form a cube, which implies that only a tetragonal phase can be formed. Vice versa, when $r_R<(1/\sqrt{3})r_T$ the representative surfaces of the rhombohedral phase will form a closed octahedron so that only a rhombohedral phase can be formed. This restricts the $\delta$ values in the following range:

$$1-\sqrt{3}<\delta<1-(1/\sqrt{3}). \tag{6}$$

For $\delta$ values out of this range, the low-temperature phase will be single phase.

Using the formula Eq. (3) the distribution functions $f_T$ and $f_R$ in terms of this single parameter $\delta$ can be obtained for the polyhedron in Figs. 5(a) and 5(b):

$$f_T=\begin{cases}\dfrac{6}{\pi}\arcsin\left(\dfrac{\sqrt{3}[2(1-\delta)-\sqrt{3}]}{2(1-\delta)^2+[\sqrt{3}-(1-\delta)]^2}\right), & 1-\sqrt{3}<\delta<1-\dfrac{2}{\sqrt{3}}\\ \dfrac{6}{\pi}\arcsin\left(\dfrac{[\sqrt{3}(1-\delta)-1]^2}{2+[\sqrt{3}(1-\delta)-1]^2}\right), & 1-\dfrac{2}{\sqrt{3}}<\delta<1-\dfrac{1}{\sqrt{3}},\end{cases} \tag{7}$$

$$f_R=1-f_T. \tag{8}$$

At the MPB we have $G_T=G_R$ or $\delta=0$, so that the probability ratio for a particle of the cubic phase to transform into the rhombohedral and tetragonal phases becomes

$$\frac{f_R}{f_T}=\frac{\pi-6\arcsin[(3-\sqrt{3})/6]}{6\arcsin[(3-\sqrt{3})/6]}\approx 1.45. \tag{9}$$

When we have an ensemble of the particles, such as a powder ceramic system, Eq. (9) represents the molar ratio of the two low-temperature phases at the MPB composition.[3]

## III. COMPARISON WITH EXPERIMENTS

Because the difference of the two free-energy densities is small near the MPB we may write it as a series expansion of the composition about the MPB composition $x_0$,

$$g_R-g_T=\frac{1}{v}(G_R-G_T)=\sum_{n=1}^{\infty}\alpha_n(x-x_0)^n, \tag{10}$$

where $v$ is the volume of the individual element in a statistical ensemble and $x_0$ is the composition at which the free energies of the two low-temperature phases become equal. Looking at Fig. 1(d) one finds that Eq. (10) may be well represented by a linear function near $x_0$,

$$g_R-g_T=\alpha_1(x-x_0). \tag{11}$$

Using this relation and Eqs. (5) and (6) we can derive the width of the coexistence region $\Delta x$,

$$\Delta x=(2kT_c/|\alpha_1|v)\ln 3. \tag{12}$$

An important conclusion can be drawn from Eq. (12): The width and the boundary compositions of the coexistence region are not well defined in a complete solid solution system, they depend on the volume $v$ of the statistical elements. This fact marks the physical difference between the phase coexistence inside a solubility gap and near the MPB of a complete solid solution system [see Figs. 1(a) and 1(c)]. A corollary from this conclusion is that the coexistence region will be infinitely sharp for a single-crystal system, but for a small-grain system the coexistence

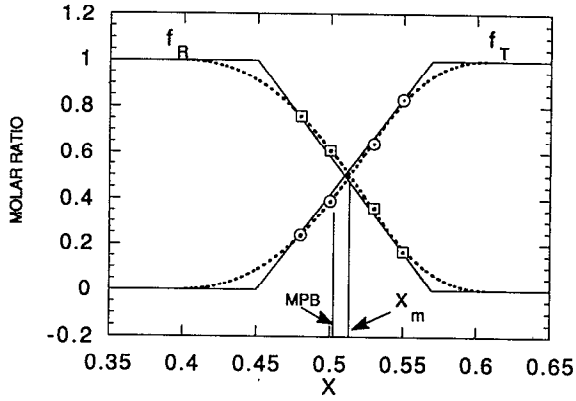


FIG. 6. Molar fractions $f_R$ and $f_T$ of the rhombohedral and tetragonal phases inside the coexistence compositional region for $0.1Pb_{0.9}K_{0.1}(Zn_{1/3}Nb_{2/3})O_{2.95}$-$(0.9-x)PbZrO_3$-$xPbTiO_3$ solid solution. The squares and circles are experimental data from Ref. 5; the solid curves were fitted using the Lever Rule, and the dotted curves were fitted using the current theory.

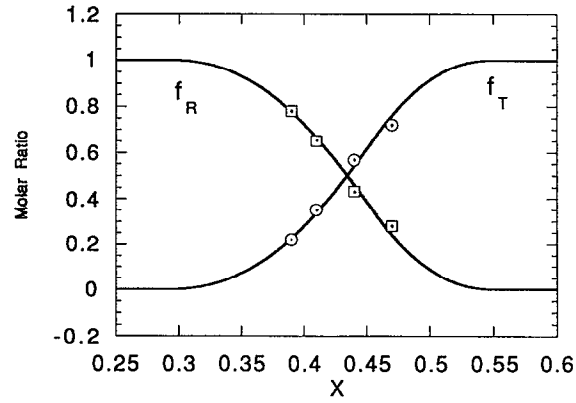


FIG. 7. Experimental data (the squares and circles) of Ari-Gur and Benguigui (Ref. 6) on the PZT system and the fitted curves using the current theory.

region will become considerably wider. For a fixed volume, if the free-energy difference of the two low-temperature phases changes drastically away from the MPB, i.e., $|\alpha_1|$ is large, there should be a very narrow coexistence region, otherwise the coexistence region could be wide.

Substituting Eq. (13) into Eq. (11) we can rewrite Eq. (5) in the following form:

$$\delta = 1 - \exp[(x - x_0)\ln 3/\Delta x]. \tag{13}$$

The parameters $x_0$ and $\Delta x$ may be fitted from experimental data using Eqs. (13) and (7) [or Eq. (8)]. Two examples are given below to demonstrate the procedures.

It is known from experience that the coexistence region in the pure PZT system is very narrow because the grain growth is difficult to control. Therefore, due to the limitations of x-ray resolution it is difficult to obtain a reliable molar ratio of the rhombohedral and tetragonal phases from x-ray-diffraction measurements. However, when small amounts of dopants are added to the PZT system (within the limit of not destroying the solid solution characteristic), the coexistence region usually becomes wider and the x-ray-diffraction peaks become relatively easier to separate from each other.

We have found two sets of experimental data in the literature. The data points in Fig. 6 were measured by Hanh, Uchino, and Nomura[5] on the complete solid solution system $0.1Pb_{0.9}K_{0.1}(Zn_{1/3}Nb_{2/3})O_{2.95}$-$(0.9-x)PbZrO_3$-$xPbTiO_3$. (Note that the compositional variable $x$ refers to the mole percent of $PbZrO_3$ in Ref. 5 but refers to the mole percent of $PbTiO_3$ in this article; all data points have been converted accordingly.) The squares and circles are the molar fractions of the rhombohedral and tetragonal phases, respectively. The authors of Ref. 5 have fitted their experimental data to the Lever Rule, which is shown in Fig. 6 as the solid curves. The two edge compositions are $x_1=0.45$ and $x_2=0.57$. Although it appears that the fitting is reasonably good for these limited data points, the kinks at $x_1$ and $x_2$ are in contradiction with the nature of a complete solid solution system. As mentioned above, the two edge compositions in the Lever Rule actually define a solubility gap, and one cannot explain the physical meaning of these two edge compositions for a complete solid solution system. The dotted curves are fitted using the theory presented in this article, and the two fitted parameters are $x_0=0.5027$ and $\Delta x=0.2066$. We can see that the fittings are surprisingly good. More important, the kinks have been smoothed out, which is more consistent with the nature of the complete solid solution systems.

In comparison the width of the coexisting region obtained from the current theory, $\Delta x=0.2066$, is wider than that given by the Lever Rule, $x_2-x_1=0.12$. Both theories agree reasonably well if the second phase has more than 20%, but they deviate severely from each other near the edges of the coexistence region. In practice, the long tails in our theory may be difficult to observe because of the limited resolution of conventional x-ray techniques. For this reason we give a useful relation to estimate the width parameter $\Delta x$,

$$\Delta x \approx 18.87\,(x_m - x_0), \tag{14}$$

where $x_0$ is the MPB composition at which $f_R{:}f_T \approx 60{:}40$, and $x_m$ is the equal fraction composition at which $f_R{:}f_T = 50{:}50$. These two compositions can be easily obtained from experiments and are indicated in Fig. 6.

Unlike the Lever Rule, the distribution functions, Eqs. (7) and (8), are asymmetric with respect to the equal fraction composition $x_m$, and one may notice this point by looking at the dotted curves in Fig. 6. This asymmetric feature has been verified by experiments in other systems, for example, the experimental results of Ari-Gur and Benguigui[6] for the PZT solid solution system (Fig. 7). One can clearly see this asymmetry from their data. Although it seems that some errors might have occurred in their experiments because the MPB composition has been shifted further to the rhombohedral side (which might be caused by the presence of impurities in their chemicals), the data can still be well fitted using Eqs. (7) and (8). The two fitted parameters are $x_0=0.4212$ and $\Delta x=0.2554$.

## IV. SUMMARY AND CONCLUSIONS

The distribution functions have been derived for the coexisting phases near the morphotropic phase boundary in a complete binary solid solution system. It is shown that the phase coexistence near the MPB in a complete solid solution is different from the phase coexistence inside a solubility gap. The latter has two special compositions $x_1$ and $x_2$ specifying the edges of a solubility gap, and the distribution inside the gap can be described by the Lever Rule. While for the former, only the MPB composition $x_0$ is well defined, the width of the coexisting region is inversely proportional to the volume of individual element in a statistical ensemble.

Explicitly, we can see the difference between the two theories through the following example. Assume we have a binary system AC-BC and assume they form solid solutions $\alpha$ and $\beta$ for A- and B-rich compounds, respectively. Then, for any given composition $x$ inside the coexistence region of $\alpha$ and $\beta$ we have the two theories describe the following situations:

(a) Lever Rule:

$$xAC+(1-x)BC=f_{\alpha}A_{x_1}B_{1-x_1}C\ (\alpha\ \text{structure})+f_{\beta}A_{x_2}B_{1-x_2}C\ (\beta\ \text{structure}),$$

(b) Present theory:

$$xAC+(1-x)BC=f_{\alpha}A_{x}B_{1-x}C\ (\alpha\ \text{structure})+f_{\beta}A_{x}B_{1-x}C\ (\beta\ \text{structure}).$$

The Lever Rule specifies a solubility gap from $x_1$ to $x_2$, and the two coexisting phases have different chemical compositions as shown on the right-hand side (rhs) of the first equation, while the current theory deals with the structural phase mixing with the same chemical composition as indicated on the rhs of the second equation. It is our belief that the observed coexisting phases in a complete solid solution system actually consist of a second metastable structure that was frozen in at the paraelectric-ferroelectric phase transition.

Compared to the Lever Rule, the current theory does not give those kinks in the distribution functions, therefore it is more consistent with the nature of a complete solid solution system (no solubility gap). The distribution functions [Eqs. (7) and (8)] are asymmetric with respect to the middle point $x_m$, which is another major difference from the Lever Rule. Experimental results show that this asymmetry indeed exists (see Figs. 6 and 7). In addition to the surprisingly good agreement between the theory and the available experimental data, the current theory also provides a reasonable explanation to the controversy regarding the width of the coexistence region in the PZT system, which has been an issue of debate since the appearance of PZT. We conclude that a well-defined width cannot exist in a complete solid solution system because $\Delta x$ is inversely proportional to the volume of the element in a given statistical ensemble, such as the grain size in a ceramic. Since the grain size depends strongly on the ceramic processing procedures, it is no surprise to see those reported experimental discrepancies regarding the width of the coexistence region.

## ACKNOWLEDGMENTS

The authors would like to thank Professor Manfred Wuttig for his constructive comments on this manuscript. This research was supported in part by the Office of Naval Research under Grant No. 00014-92-J-1510.

[1] M. J. Haun, E. Furman, S. J. Jang, and L. E. Cross, Ferroelectrics **99**, 63 (1989).
[2] V. A. Isupov, Sov. Phys. Solid State **12**, 1084 (1970).
[3] W. Cao and L. E. Cross, Jpn. J. Appl. Phys. **31**, 1399 (1992).
[4] M. J. Haun, E. Furman, H. A. McKinstry, and L. E. Cross, Ferroelectrics **99**, 27 (1989).
[5] L. Hanh, K. Uchino, and S. Nomura, Jpn. J. Appl. Phys. **17**, 637 (1978).
[6] P. Ari-Gur and L. Benguigui, Solid State Commun. **15**, 1077 (1974).